



RAPID COMMUNICATION

The single-cell landscape reveals unique tumor subsets and microenvironments associated with poor clinical outcomes in primary testicular diffuse large B-cell lymphoma



Diffuse large B cell lymphoma (DLBCL) is one of the most prevalent lymphoid malignancies. The current standard of care can cure about two-thirds of DLBCL patients.¹ Primary testicular diffuse large B-cell lymphoma (PT-DLBCL) is a rare but highly aggressive form of mature B-cell lymphoma that accounts for approximately 1%–9% of testicular malignancies. Different from nodal DLBCL, PT-DLBCL has a markedly worse prognosis because of inferior response to the current treatment regimens and significant extranodal tropism.² Three main questions remained unresolved in the field of PT-DLBCL research. Previously, two prognostically important categories of DLBCL have been defined: activated B cell-like (ABC) DLBCL and germinal center B cell-like (GCB) DLBCL. Most PT-DLBCLs were classified as ABC-DLBCL. However, the exact cells of origin (COO) of PT-DLBCL were still under debate. Secondly, the lack of transcriptomics profiling of PT-DLBCL at the single-cell level hindered the discovery of intra-tumor heterogeneity. Finally, the role of the testis microenvironment in PT-DLBCL was unclear. Herein, we performed single-cell RNA sequencing (scRNA-Seq) and bulk whole exome sequencing (WES) to reveal the molecular landscape of PT-DLBCL. We defined predictive signatures based on gene profiles of the pivotal clusters. Our study could be a benefit for the clinical classification of PT-DLBCL and provide valuable therapeutic targets.

The pooled analysis of survival data showed that PT-DLBCL patients had a dramatically worse prognosis compared with nodal DLBCL (HR = 1.1, 95% CI 1.1–1.2; $P < 0.001$), especially for the 10-year survival, indicating PT-DLBCL has high risk of late recurrence or metastasis, which prompted us to deeply investigate the underlying mechanism

(Fig. S1A, B). We comprehensively profiled the cell populations in human PT-DLBCL by single-cell RNA-seq for primary tumors resected from 3 untreated patients (Fig. S1C and Table S1). After the removal of low-quality cells, we acquired single-cell transcriptomes in a total of 30,545 cells. Different cell types were distinguished using unsupervised clustering (Fig. 1A). Based on the expression of well-known markers which were strongly and specifically marked regarding each major cell population, we annotated the cells as B cells, T cells, myeloid cells, endothelial cells, myoid cells, and germ cells (Fig. S2A–C). B cells were defined as malignant cells by the detection of copy number variation inferred by inferCNV, CopyKAT, and WES (Fig. S2D–F). Histologically, the tumors showed large atypical lymphocytes with irregular nuclei, and high levels of Ki-67 and CD20 expression (Fig. S2G). All three PT-DLBCL were classified as ABC-DLBCL using the Hans algorithm (Fig. S3).

We further reclustered 21,059 malignant B cells from all three samples into three sub-groups: germinal center B cell-like (GC-like), plasma cell-like (plasma-like), and memory B cell-like (memory-like) lymphoma cells (Fig. 1B). GC-like lymphoma cells expressed GC-related signature (Fig. 1C). Plasma-like lymphoma cells expressed known plasma cell markers (Fig. 1D). Gene set enrichment analysis (GSEA) revealed strong enrichment of memory cell signature among the transcriptome profiles of memory-like lymphoma cells (Fig. 1E). RNA velocity and trajectory analysis showed that cells from memory-like cluster constitute the cells of origin, while GC-like and plasma-like lymphoma cells mainly located at the ends of the trajectory (Fig. 1F; Fig. S4). This may be due to memory B cell reactivation during restimulation which enabled it to re-enter the germinal center reaction or differentiate into plasma cells.³ The memory-like lymphoma cells were regrouped into four clusters. Enrichment analysis revealed the functional heterogeneity

Peer review under responsibility of Chongqing Medical University.

<https://doi.org/10.1016/j.gendis.2023.02.036>

2352-3042/© 2023 The Authors. Publishing services by Elsevier B.V. on behalf of KeAi Communications Co., Ltd. This is an open access article under the CC BY-NC-ND license (<http://creativecommons.org/licenses/by-nc-nd/4.0/>).

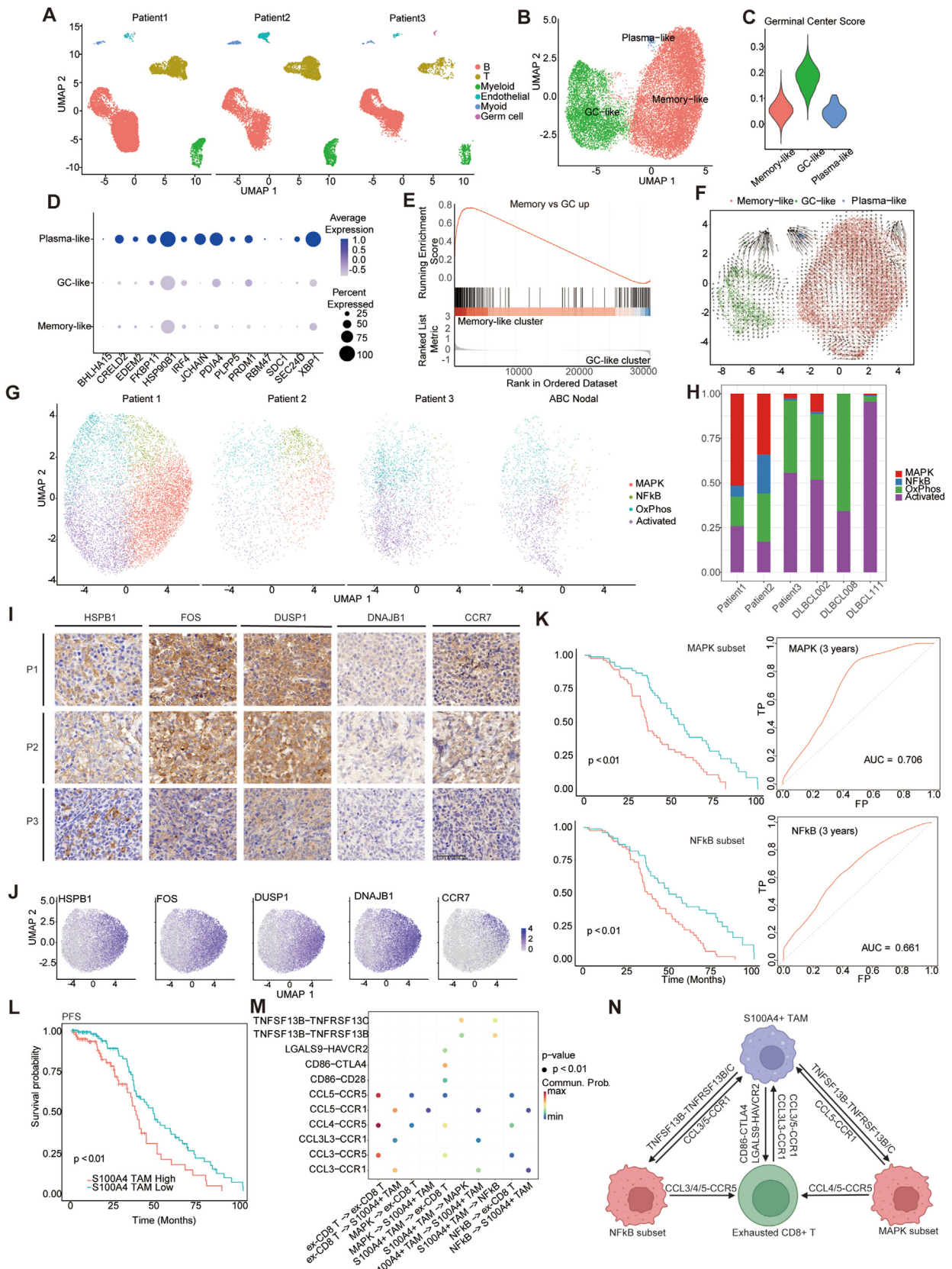


Figure 1 The single-cell landscape reveals unique tumor subsets and microenvironments associated with poor clinical outcomes in PT-DLBCL. **(A)** The UMAP plots of all cells from three samples colored by cell types and separated by patient identity number. **(B)** The UMAP plot of malignant B cells colored by three main sub-populations. **(C)** The violin plot of average scores associated with germinal center B cells for each cluster within malignant B cells. **(D)** The dot plot of the average expression of marker genes

of four subclusters (Fig. 1G). NFkB subset showed enrichment of NFkB signaling pathway genes, and MAPK subset showed activation of MAPK signaling, while both were only presented in PT-DLBCL patients with metastasis, suggesting the potential pro-metastasis property (Fig. S5). The other two subsets showed gene enrichment in the B cell activation pathway (Activated subset), and oxidative phosphorylation (OxPhos subset). To further investigate whether this heterogeneity was present in other patients, we analyzed memory-like lymphoma cells from public scRNA-seq data of nodal ABC DLBCL (ABC DLBCLn) patients.⁴ Interestingly, the NFkB and MAPK subsets are absent in ABC-DLBCLn (Fig. 1H). The signatures of these lymphoma subsets were further validated using IHC. The strong expression of DUSP1, FOS, HSPB1, DNAJB1 (markers of MAPK subset), and CCR7 (a marker of NFkB subset) was observed in patients 1 and 2 but not in patient 3 (Fig. 1I, J). We used a public dataset to validate the prognostic risk prediction model, each ABC-DLBCLn patient was scored using gene signatures highly expressed in MAPK, NFkB, Activated, and OxPhos subsets.⁵ The median of the scores was used to divide patients into high-risk and low-risk groups. Interestingly, high-risk patients identified by a 49-gene signature of MAPK subsets had worse overall survival compared with low-risk patients (Fig. 1K). A 50-gene signature of the NFkB subset was also associated with worse overall survival. The receiver operating characteristics (ROC) curve was used to evaluate the prediction power of the two gene signatures. The gene signature of the MAPK subset achieved a 3-year AUC (area under the curve) of 0.706 and a 5-year AUC of 0.640 (Fig. 1K; Fig. S6). While the ROC analysis revealed a 3-year AUC of 0.661 and a 5-year AUC of 0.649 with gene signature of NFkB subset.

We further investigated the microenvironment of PT-DLBCL (Fig. S7). Five distinct clusters were found in the myeloid lineage, including one cluster of normal testis macrophages, three clusters of tumor-associated macrophages (S100A4⁺ TAM, CCL8⁺ TAM, and SPARC⁺ TAM), and one cluster of dendritic cells (DC) (Fig. S7F). A much higher proportion of S100A4⁺ TAM was presented in PT-DLBCL with metastasis. We analyzed the public ABC DLBCLn dataset using Cibersortx and found that patients with a higher proportion of S100A4⁺ TAM had worse progression-free survival compared with those with a lower proportion (Fig. 1L). The two lymphoma subsets specifically presented in metastatic PT-DLBCL, NFkB, and MAPK subsets, recruited immune cells to the tumor microenvironment (TME) (Fig. 1M, N). Specifically, the NFkB subset recruited

S100A4⁺ TAM through CCL3/5-CCR1 interactions and recruited exhausted CD8⁺ T cells through CCL3/4/5-CCR5 interactions. MAPK subset recruited S100A4⁺ TAM through CCL5-CCR1 interactions and recruited exhausted CD8⁺ T cells through CCL4/5-CCR5 interactions.

Furthermore, S100A4⁺ TAMs recruited by lymphoma cells contributed to the exhaustion of cytotoxic CD8 T cells. While exhausted CD8 T cells further recruited TAMs into the TME. After being recruited to the lymphoma microenvironment, the activation of TNFSF13B-TNFRSF13B/C signaling between S100A4⁺ TAMs and the NFkB subset may promote the proliferation and survival of lymphoma cells. Furthermore, cell–cell signaling associated with immunosuppression such as CD86-CTLA4 and LGALS9-HAVCR2 was activated between S100A4⁺ TAMs and exhausted CD8⁺ T cells, leading to further CD8⁺ T cell exhaustion. Interestingly, exhausted CD8⁺ T cells also delivered signals to S100A4⁺ macrophages through CCL3/5-CCR1 and CCL3L3-CCR1 signaling to promote migration.

In conclusion, we provided deep insights into the cells of origin in PT-DLBCL. Pivotal malignant B cell clusters and tumor-supportive microenvironment associated with patient survival were identified and need further investigation to enable personalized treatment on advanced PT-DLBCL patients. Due to the unique characteristics, we found in PT-DLBCL, further studies should be conducted to develop more specific therapies targeting this lymphoma type.

Author contributions

Yanjie Zhang, Hengchuan Su, and Daliu Min: conceptualization; Benhong Gu, Guohai Shi, and Jiahui Guo: resources and investigation; Zhouliang Bian, Hanlin Zeng, and Yanjie Zhang: formal analysis, data curation, and visualization; Zhouliang Bian and Yanjie Zhang: writing - original draft; Hengchuan Su, Daliu Min, Bin Jiang, Hanlin Zeng, and Dong Li: writing - review & editing.

Conflict of interests

The authors have no competing interests to declare.

Funding

This work was partially supported by grants from the National Natural Science Foundation of China, China (No. 82072638 to Y.Z. and No. 81602222 to H.S.) and the Biobank

associated with plasma cells for each cluster. (E) GSEA of malignant B cells from patient 1 showed enrichment of gene signatures associated with up-regulated genes in memory B cells versus germinal center B cells in the memory-like cluster. (F) RNA velocity analysis for malignant B cells from patient 1 showed the origin of lymphoma cells in the memory-like cluster. (G) Memory-like malignant B cells from PT-DLBCL were clustered with unsupervised clustering. The clustering information was used to annotate memory-like B cells in ABC-DLBCLn from external datasets. (H) The bar plots showed the proportion of subclusters within each sample. (I) Immunohistochemical analysis of markers associated with MAPK and NFkB subsets (HSPB1, FOS, DUSP1, DNAJB1, CCR7). (J) The expression of markers (HSPB1, FOS, DUSP1, DNAJB1, CCR7) in scRNA-seq data from three PT-DLBCL patients. (K) Survival analysis examined the association between genes associated with MAPK and NFkB clusters and the survival of ABC-DLBCLn patients. The ROC curve was used to evaluate the prediction power of the two gene signatures derived from MAPK and NFkB subsets. (L) A higher proportion of S100A4⁺ TAM was associated with worse PFS. (M) The bubble plot showing ligand–receptor pairs between important cell populations (ex-CD8 T: exhausted CD8⁺ T cell). (N) The schematic diagram of cell-to-cell interaction which may contribute to PT-DLBCL and its progression.

Program of Shanghai Ninth People's Hospital, Shanghai Jiao Tong University School of Medicine, Shanghai, China (No. YBKB202217 to Y.Z.).

Data availability

All scRNA-seq and WES data presented here are available at Genome Sequence Archive (accession number: HRA002975).

Acknowledgements

We thank Li Zhang and Qin Yang for their help in this project. The results here are partly based upon data generated by the TCGA Research Network (<https://www.cancer.gov/tcga>) and the GEO database (<https://www.ncbi.nlm.nih.gov/geo/>).

Appendix A. Supplementary data

Supplementary data to this article can be found online at <https://doi.org/10.1016/j.gendis.2023.02.036>.

References

- Pollari M, Leivonen SK, Leppä S. Testicular diffuse large B-cell lymphoma-clinical, molecular, and immunological features. *Cancers*. 2021;13(16):4049.
- Takahashi H, Tomita N, Yokoyama M, et al. Prognostic impact of extranodal involvement in diffuse large B-cell lymphoma in the rituximab era. *Cancer*. 2012;118(17):4166–4172.
- Venturutti L, Melnick AM. The dangers of déjà vu: memory B cells as the cells of origin of ABC-DLBCLs. *Blood*. 2020;136(20):2263–2274.
- Steen CB, Luca BA, Esfahani MS, et al. The landscape of tumor cell states and ecosystems in diffuse large B cell lymphoma. *Cancer Cell*. 2021;39(10):1422–1437.
- Xu-Monette ZY, Møller MB, Tzankov A, et al. MDM2 phenotypic and genotypic profiling, respective to TP53 genetic status, in diffuse large B-cell lymphoma patients treated with rituximab-CHOP immunochemotherapy: a report from the International DLBCL Rituximab-CHOP Consortium Program. *Blood*. 2013;122(15):2630–2640.

Zhouliang Bian ^{a,b,1}, Benhong Gu ^{c,1}, Guohai Shi ^{d,e,1}, Jiahui Guo ^{a,b}, Dong Li ^c, Hanlin Zeng ^{a,b}, Bin Jiang ^{a,****}, Dalu Min ^{f,***}, Hengchuan Su ^{d,e,**}, Yanjie Zhang ^{a,b,*}

^a Department of Oncology, Ninth People's Hospital, Shanghai Jiao Tong University School of Medicine, Shanghai 201900, China

^b Shanghai Institute of Precision Medicine, Ninth People's Hospital, Shanghai Jiao Tong University School of Medicine, Shanghai 200125, China

^c Department of Urology, Tongren Hospital, Shanghai Jiao Tong University School of Medicine, Shanghai 200336, China

^d Department of Urology, Fudan University Shanghai Cancer Center, Shanghai 200032, China

^e Department of Oncology, Shanghai Medical College, Fudan University, Shanghai 200032, China

^f Department of Oncology, Shanghai Jiao Tong University Affiliated Sixth People's Hospital, Shanghai 200233, China

*Corresponding author. Department of Oncology, Ninth People's Hospital, Shanghai Jiao Tong University School of Medicine, Shanghai 201900, China.

**Corresponding author. Department of Urology, Fudan University Shanghai Cancer Center, Shanghai 200032, China.

***Corresponding author.

****Corresponding author.

E-mail addresses: jiangbinwcr@163.com (B. Jiang), docmin1969@sjtu.edu.cn (D. Min), suhengchuan@163.com (H. Su), zhangyanjie@shsmu.edu.cn (Y. Zhang)

9 October 2022
Available online 19 April 2023

¹ These authors contributed equally to this work.